# scientific reports



## **OPEN**

# Image quality and radiation dose of reduced-dose abdominopelvic computed tomography (CT) with silver filter and deep learning reconstruction

Chuluunbaatar Otgonbaatar<sup>1,2</sup>, Sang-Hyun Jeon³, Sung-Jin Cha³, Hackjoon Shim²,<sup>4</sup>, Jin Woo Kim³ & Jhii-Hyun Ahn³<sup>⊠</sup>

To assess the image quality and radiation dose between reduced-dose CT with deep learning reconstruction (DLR) using SilverBeam filter and standard dose with iterative reconstruction (IR) in abdominopelvic CT. In total, 182 patients (mean age ± standard deviation, 63 ± 14 years; 100 men) were included. Standard-dose scanning was performed with a tube voltage of 100 kVp, automatic tube current modulation, and IR reconstruction, whereas reduced-dose scanning was performed with a tube voltage of 120 kVp, a SilverBeam filter, and DLR. Additionally, a contrast-enhanced (CE)-boost image was obtained for reduced-dose scanning. Radiation dose, objective, and subjective image analyses were performed in each body mass index (BMI) category. The radiation dose for SilverBeam with DLR was significantly lower than that of standard dose with IR, with an average reduction in the effective dose of 59.0% (1.87 vs. 4.57 mSv). Standard dose with IR (10.59 ± 1.75) and SilverBeam with DLR  $(10.60 \pm 1.08)$  showed no significant difference in image noise (p = 0.99). In the obese group (BMI > 25 kg/ m<sup>2</sup>), there were no significant differences in SNRs of the liver, pancreas, and spleen between standard dose with IR and SilverBeam with DLR. SilverBeam with DLR + CE-boost demonstrated significantly better SNRs and CNRs, compared with standard dose with IR and SilverBeam with DLR. DLR combined with silver filter is effective for routine abdominopelvic CT, achieving a clearly reduced radiation dose while providing image quality that is non-inferior to standard dose with IR.

**Keywords** Reduced-dose CT, Abdominopelvic CT, Image quality, Deep learning image reconstruction, SilverBeam filter

Abdominopelvic computed tomography (CT) is widely used to diagnose abdominal pathology, monitor treatment response, detect tumor recurrence, and conduct follow-up assessments<sup>1</sup>. However, repeated CT examinations of the abdomen increase the cumulative radiation dose, thereby heightening the risk of radiation-related adverse effects for patients<sup>2,3</sup>. Increased awareness of radiation exposure has led to widespread interest in optimizing radiation doses while maintaining image quality. Therefore, techniques have been developed and applied to reduce radiation dose, such as lower tube voltage, automatic tube current modulation, deep learning reconstruction (DLR), and size-specific protocols<sup>4–7</sup>. The use of a low tube voltage and tube current significantly reduces radiation exposure but substantially increases image noise<sup>8–10</sup>. Iterative reconstruction (IR) with a low-dose setting decreases image noise, compared with traditional filtered-back projection with a standard dose setting, but reduces the detectability of low-contrast lesions<sup>11,12</sup>.

Furthermore, recent developments in image reconstruction, including model-based IR (MBIR) and DLR, have led to decreased image noise, even in low-dose CT settings. Several studies have investigated the superior performance of MBIR over IR for detecting small liver lesions <sup>13,14</sup>. However, the long reconstruction time limits

<sup>1</sup>Department of Radiology, College of Medicine, Seoul National University, Seoul, Republic of Korea. <sup>2</sup>Medical Imaging AI Research Center, Canon Medical Systems Korea, Seoul, Republic of Korea. <sup>3</sup>Department of Radiology, Wonju Severance Christian Hospital, Yonsei University Wonju College of Medicine, 20 Ilsan-ro, Wonju, Gangwon-do 26426, Republic of Korea. <sup>4</sup>ConnectAI Research Center, Yonsei University College of Medicine, Seoul, Republic of Korea. <sup>≅</sup>email: radajh@yonsei.ac.kr

its widespread use in routine practice<sup>15</sup>. Conversely, compared with IR and MBIR, DLR potentially improves image quality by reducing image noise and increasing the signal-to-noise ratio (SNR) and contrast-to-noise ratio (CNR) through a deep convolutional neural network<sup>16,17</sup>. It is critical to balance radiation dose and CT image quality.

Tin filtration has been proposed as another approach for decreasing radiation exposure by absorbing low-energy photons. Studies have demonstrated the beneficial role of tin filtration in dose reduction, with similar diagnostic performance and image quality to the standard dose protocol 18,19. The silver filter is a newly introduced method that elevates the average energy level, eliminates low-energy photons, and shifts the spectral peak toward a higher-energy range. These changes remove the low-energy photons 20,21. Contrast-enhanced (CE)-boost is a noninvasive method that increases the degree of vascular contrast without increasing the concentration or delivery rate of the iodinated contrast media. Studies on CE-boost have evaluated the image quality and diagnostic performance of the abdominal aorta and pulmonary vessels, compared with conventional images 22-25. To the best of our knowledge, no study has investigated the effects of DLR and CE-boost with a SilverBeam filter on the evaluation of image quality in abdominopelvic CT. Therefore, in this study, we aimed to assess the image quality and radiation dose between reduced-dose CT with DLR using a SilverBeam filter and standard dose with IR in abdominopelvic CT.

# Materials and methods Patient population

This retrospective study was approved by the Institutional Review Board of Wonju Severance Christian Hospital (IRB number: CR324085) with a waiver of informed consent. All methods were performed following the Declaration of Helsinki. This study included two patient groups. The first group consisted of 93 patients who underwent abdominopelvic CT at a reduced dose setting using a SilverBeam filter from May 2024 to July 2024. The second group included 93 age-, sex-, and body mass index (BMI)-matched patients who underwent abdominopelvic CT at standard-dose settings from May 2024 to June 2024. The exclusion criterion was incomplete image reconstruction due to loss of raw projection data (n=1) and motion artifact (n=3). BMI was determined by dividing weight in kilograms by the square of height in meters. Radiation dose and image quality were compared among three patient groups based on BMI:  $< 20, 20-24.9, and \ge 25 \text{ kg/m}^2$  26.

### Abdominopelvic CT imaging protocol

For standard-dose CT, images were acquired using a multidetector CT scanner (SOMATOM Force; Siemens Healthineers, Erlangen, Germany). The imaging parameters were as follows: tube voltage, 100 kVp; gantry rotation time, 500 ms; detector collimation, 192×0.6 mm; and slice thickness, 3 mm. Automated tube current modulation (CareDose4D; Siemens Healthineers, Erlangen, Germany) was used to activate the tube current. The standard-dose setting images were obtained using an advanced modeled IR–soft convolution kernel (Br40d) (ADMIRE, Siemens Healthineers, Erlangen, Germany).

All patients in the reduced-dose setting underwent imaging using a multidetector CT scanner (Aquilion ONE PRISM, Canon Medical Systems Corporation, Otawara-shi, Japan) $^{27}$ . The imaging parameters were as follows: tube voltage, 120 kVp; gantry rotation time, 600 ms; detector collimation  $80 \times 0.5$  mm; slice thickness, 3 mm; and SilverBeam filter. An automatic exposure control (SUREExposure; Canon Medical Systems Corporation, Otawara-si, Japan) was used to measure the tube current. The reduced-dose setting images were obtained using DLR with the body sharp option and standard strength (Advanced Intelligent Clear IQ Engine, Canon Medical Systems Corporation, Otawara-shi, Japan).

In addition, CE-boost images were generated for Silver Beam using DLR. CE-boost images were obtained by adding CE and iodinated images, which were subtracted from non-contrast and CE images during postprocessing (Fig. 1).

All images were obtained in the craniocaudal direction from the dome of the diaphragm to the inferior margin of the pubic symphysis. Portal venous phase imaging was started 70 s after injecting 95 mL of a nonionic iodinated contrast agent (Iohexol 350, GE Healthcare, Milwaukee, Wisconsin) at a rate of 2.3 mL/s with an automatic bolus-tracking program (SUREStart, Canon Medical Systems Corporation) in the ascending aorta (trigger threshold level, 100 Hounsfield units [HUs]). The contrast agent was administered through the antecubital vein, using a dual-head power injector (Dual Shot Alpha 7; Nemoto Kyorindo Co., Ltd., Japan).

The CT dose index volume  $(CTDI_{vol})$  and dose length product (DLR) were recorded. The effective dose (ED) was calculated by multiplying the DLR by the conversion coefficient for the abdomen–pelvis  $(0.015 \text{ mSv} \times \text{mGy}^{-1} \times \text{cm}^{-1})^{28}$ .

### Objective analysis

Background image noise was evaluated as the standard deviation (SD) of HU by placing a 50 mm² region of interest (ROI) in the homogeneous subcutaneous fat tissue of the anterior abdomen. CT attenuation (HU) of the liver (lateral and medial segments of the left lobe and anterior and posterior segments of the right lobe at the level of the main portal vein), pancreas (body and tail), spleen, abdominal aorta at the level of the celiac artery, and paraspinal muscles were measured. For each site, two ROIs were recorded while avoiding the inclusion vessel, bile duct, focal lesions, artifacts, calcification, and pancreatic duct, and the average value of the two ROIs was used for analysis. SNR and CNR were calculated using the following formulas:

$$\text{SNR} = \frac{HU_{organ}}{SD_{organ}}; CNR = \frac{HU_{organ} - HU_{paraspinal muscle}}{Imagenoise}$$

# Standard-dose CT with IR Non-contrast CT Non-contrast CT Non-contrast CT Contrast-enhanced CT Contrast-enhanced CT Contrast-enhanced CT Contrast-enhanced CT Contrast-enhanced CT Contrast enhancement boost Combination

**Fig. 1.** Study flowchart. The control group consisted of patients who underwent abdominopelvic CT at a standard dose setting with IR. In contrast, the reduced dose group included patients who underwent abdominopelvic CT at a reduced dose setting using the SilverBeam filter in combination with DLR. Additionally, in the reduced-dose CT group, CE-boost images were obtained by integrating the CE images with subtracted images. These subtracted images were generated through postprocessing by subtracting the non-contrast images from the CE images. *CT* computed tomography; *IR* iterative reconstruction; *DLR* deep learning reconstruction; *CE* contrast-enhanced.

### Subjective analysis

Two reviewers with 14 and 11 years of experience in abdominopelvic and general radiology, respectively, independently performed the qualitative image analysis. Both readers were blinded to the image reconstruction methods and scanners. Two readers were allowed to adjust the window level and width and randomly perform the image quality in the whole volume data using a five-point Likert scale: 5 points (excellent overall image quality, minimal image noise, no artifacts, and sufficient diagnostic confidence), 4 points (good overall image quality, mild image noise, minimal artifacts, and good diagnostic acceptability), 3 points (moderate overall image quality, moderate image noise and artifacts, and diagnosis possible), 2 points (poor overall image quality, severe image noise and artifacts, and limited diagnosis possible), and 1 point (very poor overall image quality, very severe image noise and artifacts, and not diagnostically evaluable).

### Statistical analyses

Data normality was assessed using the Kolmogorov–Smirnov and Shapiro–Wilk tests. Age and radiation dose were compared between standard- and reduced-dose CT using an independent sample *t*-test. Differences between the two protocols in terms of sex and BMI were analyzed using the chi-squared test. Image noise, SNR, CNR, CT attenuation, and subjective image analysis were compared between standard-dose CT with IR, SilverBeam with DLR, and SilverBeam with DLR+CE-boost, using one-way analysis of variance. Tukey's test was used for post hoc pairwise comparisons. Interobserver agreement was assessed with Cohen's kappa coefficient (*k*), with values interpreted as follows: <0.20 indicating poor agreement; 0.21–0.40, fair agreement; 0.41–0.60, moderate agreement; 0.61–0.80, substantial agreement; and 0.81–0.10, near-perfect agreement. *P* < 0.05 was considered statistically significant. All statistical analyses were performed using the SPSS statistical software version 25.0 (IBM, Armonk, NY, USA).

### Results

In total, 182 patients (mean age  $\pm$  SD, 63.36  $\pm$  14.49 years; 100 men) were included in this study. Demographic characteristics are shown in Table 1. There were no significant differences between the standard-dose CT and reduced-dose setting groups in terms of age (p = 0.08), sex (p = 0.99), or BMI (p = 0.93).

### Radiation dose

For each BMI group, Table 2 presents the comparative results of radiation doses between standard dose with IR and SilverBeam with DLR. The radiation dose for SilverBeam with DLR was significantly lower than that of standard dose with IR, with an average reduction in the effective dose (ED) of 59.0% (1.87 vs. 4.57 mSv), with

	Standard dose with IR (n=91)	SilverBeam with DLR (n=91)	P value
Age, years	65.3 ± 13.5	61.5 ± 15.3	0.08
Gender, males	49 (53.8%)	51 (56.0%)	0.99
BMI, kg/m <sup>2</sup>	23.91 ± 3.65	23.90 ± 3.72	0.93
BMI≥25, n	32	31	
BMI 24.9-20, n	47	48	
BMI < 20, n	12	12	
AP size, cm	21.6±3.33	20.8 ± 3.47	0.13
Lateral size, cm	31.5 ± 3.39	31.4±3.72	0.90

**Table 1**. Demographic of the patient population. Data are reported as mean  $\pm$  standard deviation. Unless otherwise indicated, the data represent the number of patients, with percentages in parentheses. *BMI* body mass index; *IR* iterative reconstruction; *DLR* deep learning reconstruction; *AP* anteroposterior.

	Standard dose with IR	SilverBeam with DLR	P value	
CTDI <sub>vol</sub> , mGy	5.59 ± 2.10	2.28 ± 0.76	0.001	
BMI≥25	6.87 ± 2.23	3.01 ± 0.72	0.001	
BMI 24.9-20	5.04 ± 1.79	2.01 ± 0.40	0.001	
BMI < 20	4.31 ± 0.73	1.45 ± 0.17	0.001	
DLP, mGy·cm	304.92 ± 124.93	131.50±51.96	0.001	
BMI≥25	383.17 ± 132.21	180.02 ± 51.58	0.001	
BMI 24.9-20	272.54 ± 105.75	113.76 ± 28.27	0.001	
BMI < 20	223.01 ± 45.22	77.11 ± 13.60	0.001	
ED, mSv	4.57 ± 1.87	1.87 ± 0.77	0.001	
BMI≥25	5.74±1.98	2.70 ± 0.77	0.001	
BMI 24.9-20	4.09 ± 1.58	1.71 ± 0.42	0.001	
BMI < 20	3.34±0.67	1.15 ± 0.20	0.001	

**Table 2**. The results of radiation dose among different CT protocols. Significant values are in bold, italics, bolditalics. Data are reported as mean  $\pm$  standard deviation. *BMI* body mass index; *IR* iterative reconstruction; *DLR* deep learning reconstruction; *CTDI*<sub>vol</sub> CT dose index volume; *DLP* dose length product; *ED* effective dose.

52.9% reduction for the BMI > 25 kg/m² group (2.70 vs. 5.74 mSv), 58.1% reduction for the 24.9–20 kg/m² BMI group (1.71 vs. 4.09 mSv), and 65.5% reduction for the BMI < 20 kg/m² group (1.15 vs. 3.34 mSv) (p < 0.001).

### Objective image analysis

With an average 59.0% lower radiation dose, there were significant differences in image noise in HU between standard dose with IR ( $10.59\pm1.75$ ), SilverBeam with DLR ( $10.60\pm1.08$ ), and SilverBeam with DLR + CE-boost ( $7.40\pm1.29$ ) (p<0.001) (Table 3). Within each BMI group, pairwise comparisons of noise between standard dose with IR and SilverBeam with DLR showed no significant differences (p=0.99). In contrast, SilverBeam with DLR + CE-boost showed significantly lower image noise, compared with both standard dose with IR and SilverBeam with DLR (p<0.001) for each BMI group.

SilverBeam with DLR resulted in significantly lower CT attenuation in the liver (p<0.001), pancreas (p<0.001), spleen (p<0.001), and abdominal aorta (p<0.001), compared with standard dose with IR. However, CT attenuation of the paraspinal muscle was comparable (p=0.11) between the two protocols (Table 3).

Overall, standard dose of IR resulted in significantly higher SNRs in the liver (p < 0.001), pancreas (p < 0.001), spleen (p < 0.001), and abdominal aorta (p < 0.001), compared with SilverBeam with DLR (Fig. 2). However, in the obesity group (BMI > 25 kg/m²), there were no significant differences in the SNRs of the liver ( $8.32 \pm 1.56$  vs.  $7.87 \pm 0.69$ , p = 0.311), pancreas ( $7.82 \pm 1.80$  vs.  $7.43 \pm 1.23$ , p = 0.577), and spleen ( $10.69 \pm 2.10$  vs.  $10.11 \pm 1.21$ , p = 0.373) between standard dose with IR and SilverBeam with DLR. For all BMI categories, SilverBeam with DLR + CE-boost demonstrated significantly improved SNRs in the liver (p < 0.001), pancreas (p < 0.001), spleen (p < 0.001), and abdominal aorta (p < 0.001), compared with standard dose with IR and SilverBeam with DLR. Although the CNRs of all structures were significantly (p < 0.001) higher for standard dose with IR than for SilverBeam with DLR across all BMI categories, SilverBeam with DLR + CE-boost yielded a significantly (p < 0.001) higher CNR than did standard dose with IR, even in the obesity group (BMI > 25 kg/m²) (Fig. 3).

### Subjective image analysis

Table 4 shows the results of the subjective image analysis comparing different CT protocols: standard dose with IR, SilverBeam with DLR, and SilverBeam with DLR+CE-boost. Both observers rated SilverBeam with

	Standard dose with IR	SilverBeam with DLR	SilverBeam with DLR+CE-boost	P value	P1 vs. P2	P1 vs. P3	P2 vs. P3	
Image noise (HU)								
Mean	10.59 ± 1.75	10.60 ± 1.08	$7.40 \pm 1.29$	0.001	0.99	0.001	0.001	
BMI≥25	10.42 ± 1.70	10.28 ± 1.12	$7.30 \pm 1.48$		0.92	0.001	0.001	
BMI 24.9-20	10.73 ± 1.89	10.63 ± 0.99	7.54 ± 1.24		0.94	0.001	0.001	
BMI < 20	10.46 ± 1.31	11.17 ± 1.13	$7.09 \pm 0.96$		0.34	0.001	0.001	
CT attenuation (HU)	CT attenuation (HU)							
Liver (mean)	119.4 ± 18.46	92.26 ± 11.30	110.11 ± 14.11	0.001	0.99	0.001	0.001	
BMI≥25	107.16 ± 15.90	86.59 ± 7.56	103.59 ± 10.21		0.92	0.001	0.001	
BMI 24.9-20	128.84 ± 16.95	93.07 ± 11.88	110.73 ± 14.55		0.94	0.001	0.001	
BMI < 20	130.64 ± 13.09	103.59 ± 7.21	124.49 ± 9.34		0.34	0.001	0.001	
Pancreas (mean)	106.5 ± 17.88	87.12 ± 13.25	108.2 ± 17.16	0.001	0.001	0.76	0.001	
BMI≥25	99.58 ± 16.30	84.10 ± 9.80	103.68 ± 14.30		0.001	0.541	0.001	
BMI 24.9-20	109.30 ± 18.02	88.32 ± 14.81	110.45 ± 18.49		0.001	0.949	0.001	
BMI < 20	114.08 ± 16.47	90.12 ± 13.90	111.01 ± 17.33		0.002	0.896	0.01	
Spleen (mean)	135.6 ± 22.29	113.80 ± 15.86	143.90 ± 20.84	0.001	0.001	0.01	0.001	
BMI≥25	130.83 ± 21.54	109.56 ± 13.21	139.04 ± 18.68		0.001	0.246	0.001	
BMI 24.9-20	137.97 ± 22.98	116.57 ± 17.29	147 ± 21.47		0.001	0.123	0.001	
BMI < 20	138.81 ± 21.10	113.45 ± 14.80	143.69 ± 22.83		0.007	0.851	0.003	
Abdominal aorta (mean)	187.90 ± 29.66	138.0 ± 32.33	191.0 ± 45.69	0.001	0.001	0.84	0.001	
BMI≥25	179.49 ± 30.11	133.79 ± 29.68	184.72 ± 40.15		0.001	0.829	0.001	
BMI 24.9-20	192.03 ± 28.77	143.26 ± 35.65	198.33 ± 51.43		0.001	0.741	0.001	
BMI < 20	194.47 ± 29.12	127.92 ± 20.95	178.02 ± 29.16		0.001	0.366	0.001	
Paraspinal muscle (mean)	60.11 ± 9.65	59.44 ± 8.04	62.08 ± 8.47	0.11	0.11	0.87	0.28	
BMI≥25	58.04 ± 10.39	56.90 ± 9.53	59.61 ± 9.96		0.893	0.814	0.522	
BMI 24.9-20	61.06 ± 8.67	59.86 ± 6.97	62.48 ± 7.39		0.740	0.668	0.180	
BMI < 20	61.85 ± 11.10	64.31 ± 5.34	66.83 ± 6.31		0.772	0.387	0.551	

**Table 3**. The results of image noise and attenuation among different image protocols. Data are reported as mean  $\pm$  standard deviation. *BMI* body mass index; *IR* iterative reconstruction; *DLR* deep learning reconstruction; *CTDI*<sub>vol</sub> CT dose index volume; *DLP* dose length product; *ED* effective dose; *HU* Hounsfield unit.

DLR as comparable to SilverBeam with DLR and standard-dose CT with IR in terms of overall image quality (p=0.320 and p=0.980), image noise (p=0.570 and p=0.990), artifacts (p=0.070 and p=0.999), and diagnostic acceptability (p=0.999 and p=0.970). Observer 2 found no significant difference in artifacts (p=0.811) and diagnostic acceptability (p=0.970) between SilverBeam with DLR+CE-boost and standard dose with IR. In contrast, observer 1 rated SilverBeam with DLR+CE-boost as inferior to standard-dose CT with IR regarding artifacts and diagnostic acceptability, primarily due to the presence of spotty high-density artifacts in the bowels (p<0.001) (Fig. 4). The interobserver agreement reached a k value of 0.24, indicating fair agreement.

### Discussion

Our study found that SilverBeam with DLR provided comparable image quality while markedly reducing the radiation dose by an average of 59.0% on abdominopelvic CT, compared with standard-dose CT with IR, in each BMI group. Additionally, the use of CE-boost with SilverBeam with DLR resulted in significantly higher image quality in terms of image noise, SNR, CNR, and subjective image analysis, compared with standard-dose CT with IR.

Several studies have reported the significant association between radiation dose and cancer risk<sup>29,30</sup>. Therefore, reducing radiation exposure while maintaining image quality and diagnostic performance is crucial, particularly in patients requiring repetitive imaging. Silver filtering is a newly introduced method that potentially offers significantly lower radiation doses. In this study, the application of a silver filter achieved an average reduction in the ED of 59.0%, with specific reductions of 52.9% for patients with a BMI > 25 kg/m², 58.1% for those with a BMI of 24.9–20 kg/m², and 65.5% for patients with a BMI < 20 kg/m², compared with the standard dose. Recent studies have compared the image quality and radiation dose between DLR with a silver filter and hybrid IR without a silver filter during chest CT scanning<sup>21,31</sup>. Golbus et al. showed an 85.5% reduction in the radiation dose for DLR with a silver filter (0.33 mSv) compared with hybrid IR without a silver filter (2.27 mSv)<sup>31</sup>. Kawamoto et al. showed that silver filters decreased image noise and improved streak artifacts, compared with images without silver filters<sup>21</sup>. Additionally, the silver filter allowed the detection of nodules in the lung and improved the image quality in terms of both the SNR and CNR, compared with the conventional copper filter used in X-ray systems<sup>20</sup>. Both studies have suggested that DLR with a silver filter potentially reduces

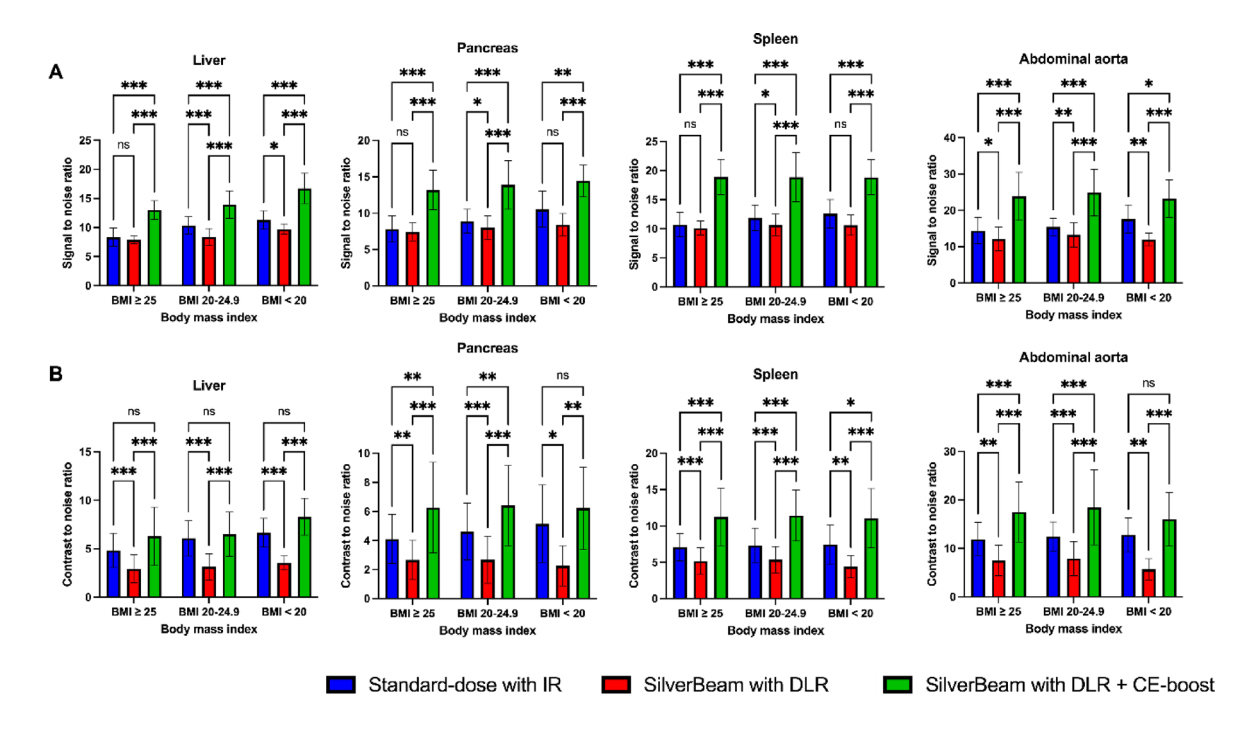


**Fig. 2.** Results of signal-to-noise ratio (SNR) and contrast-to-noise ratio (CNR). (**A**) There were no significant differences in the SNRs of the liver (p = 0.311), pancreas (p = 0.577), and spleen (p = 0.373) between standard dose with IR and SilverBeam with DLR. For all BMI categories, the SilverBeam with DLR + CE-boost demonstrated significantly improved SNRs in the liver (p < 0.001), pancreas (p < 0.001), spleen (p < 0.001), and abdominal aorta (p < 0.001), compared with standard dose with IR and SilverBeam with DLR. (**B**) SilverBeam with DLR + CE-boost yielded a significantly (p < 0.001) higher CNR than did standard dose with IR, even in the obesity group (BMI > 25 kg/m<sup>2</sup>). \*\*\*p < 0.001, \*\*p < 0.002, \*p < 0.003, ns indicates p > 0.05. *BMI* body mass index; *IR* iterative reconstruction; *CE* contrast-enhanced; *DLR* deep learning reconstruction.

radiation dose. However, no studies have investigated the effects of image quality and radiation dose using DLR with a silver filter in abdominopelvic CT.

A sufficient radiation dose is required for abdominopelvic CT, where the density difference between solid organs is smaller, unlike chest CT. Nicolan et al. studied the diagnostic performance of ultra-low-dose CT with IR for the diagnosis of non-traumatic abdominal emergencies, compared with standard-dose CT<sup>27</sup>. However, the findings of their study demonstrated a lower radiation dose (CTDI $_{vol}$  = 2.2 mGy) with the use of a low tube current (55 mAs) for ultra-low-dose CT but were insufficient for decision-making management with significantly higher image noise. Adjustment of the tube current has a straightforward linear effect on the radiation dose compared with the tube voltage. However, reducing the tube current is associated with higher image noise<sup>4</sup>. In this study, SilverBeam with DLR resulted in a significantly (p < 0.001) lower radiation dose, with a CTDI<sub>vol</sub> of 2.28 mGy, compared with standard dose with IR (CTDI<sub>vol</sub> = 5.59 mGy). Furthermore, unlike a previous study by Nicolan et al.<sup>27</sup>, there were no significant differences in image noise between reduced-dose CT with IR and standarddose CT with DLR. These results emphasize the strength of the SilverBeam filter in abdominopelvic CT with DLR over tube current modulation for reducing the radiation dose. Additionally, Tamura et al. compared the radiation dose and image quality between low-dose CT with DLR and routine-dose CT with hybrid IR<sup>32</sup>. Their study found that low-dose CT with DLR (6.9 mSv) provided superior image quality, compared with standarddose CT with IR (11.6 mSv), while achieving a 40.0% reduction in radiation dose for patients with obesity. In our study, even in patients with obesity (BMI > 25 kg/m<sup>2</sup>), the reduced radiation dose protocol (1.87 mSv) resulted in image noise and SNR comparable to that of standard-dose CT with IR. Both observers also noted non-inferior image quality for SilverBeam with DLR compared with standard dose with IR.

The present study demonstrated significantly lower CT attenuation of the liver, pancreas, spleen, and abdominal aorta when using Silver Beam with DLR compared with standard dose with IR. The standard-dose CT setting in this study was 100 kVp rather than 120 kVp with a SilverBeam filter. Despite the higher CT attenuations of the liver, spleen, pancreas, and abdominal aorta with the lower tube voltage setting for standard-dose CT, CE-boost imaging resulted in CT attenuation comparable to that of the standard dose setting (120 kVp tube voltage). Moreover, the combination of CE-boost and SilverBeam with DLR significantly improved image noise, SNR, and CNR, compared with standard-dose CT with IR. The CE-boost technique is particularly beneficial for patients with renal impairment and those who require a small amount of iodine contrast material. Hou et al. obtained lower image noise, higher CT attenuation, and greater SNR and CNR with a CE-boost in routine contrast-enhanced abdominal CT with a lower concentration of iodine contrast agent<sup>33</sup>. However, observers rated lower scores on CE-boost with the SilverBeam with DLR regarding diagnostic acceptability and

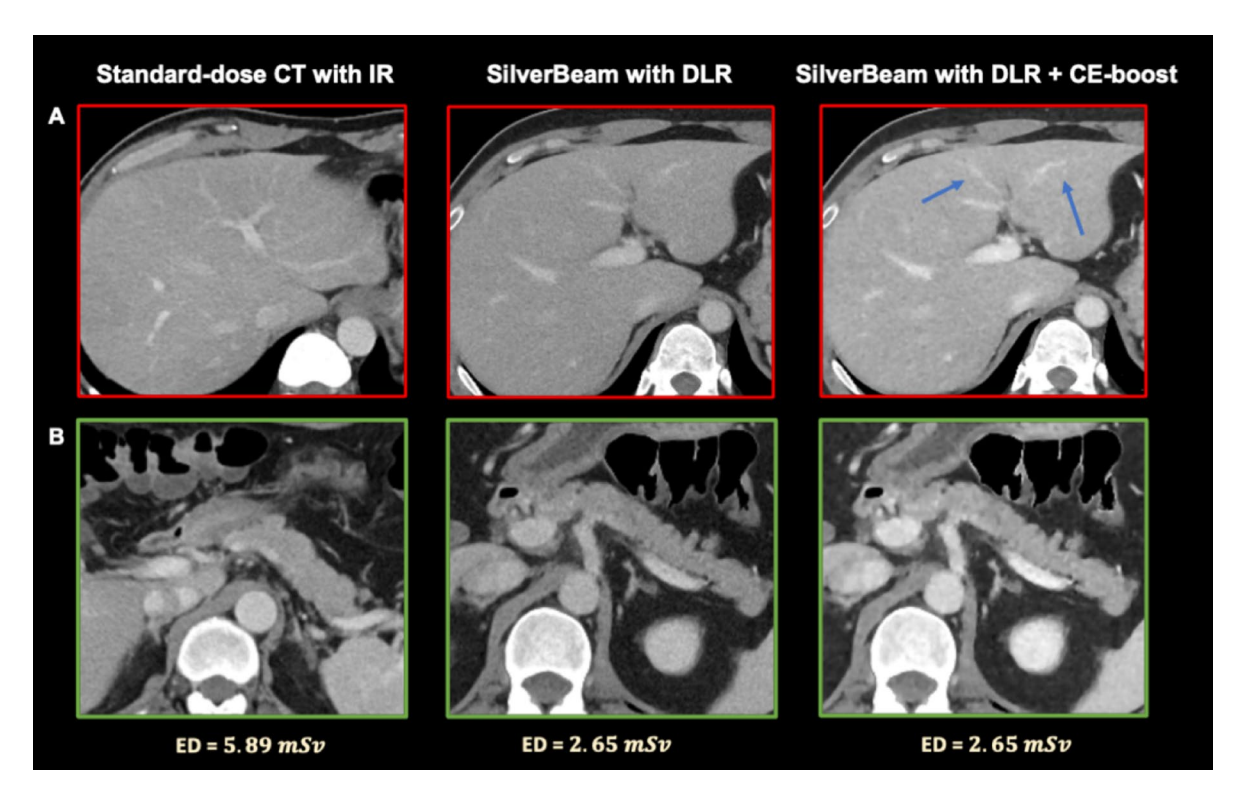


**Fig. 3.** Comparison between standard-dose and reduced-dose protocol in abdominopelvic computed tomography (CT). A 43-year-old man with a body mass index of 25.3 kg/m² underwent a standard-dose CT with IR, resulting in an effective dose of 5.89 mSv. A 46-year-old man, also with a body mass index of 25.3 kg/m², was scanned using the SilverBeam with DLR, achieving an effective dose of 2.65 mSv. CT images acquired with SilverBeam with DLR showed a significant reduction in radiation dose while maintaining the image quality, providing comparable anatomical delineation of the liver (a) and pancreatic body and tail (b). In addition, DLR + CE-boost allowed better visualization of vascular (blue arrows), compared with non-CE images. *IR* iterative reconstruction; *DLR* deep learning reconstruction; *CE* contrast-enhanced; *ED* effective dose.

	Standard dose with IR	SilverBeam with DLR	SilverBeam with DLR + CE-boost	P value	P1 vs. P2	P1 vs. P3	P2 vs. P3
Observer 1	Observer 1						
Overall image quality	4.91 ± 0.28	4.96 ± 0.17	4.62 ± 0.58	0.001	0.320	0.001	0.001
Image noise	$4.78 \pm 0.41$	4.84 ± 0.39	4.84 ± 0.39	0.510	0.570	0.570	0.999
Artifact	4.77 ± 0.42	4.94 ± 0.22	4.44 ± 0.82	0.001	0.070	0.001	0.001
Diagnostic acceptability	4.98 ± 0.10	4.99 ± 0.10	4.70 ± 0.50	0.001	0.999	0.001	0.001
Observer 2							
Overall image quality	4.93 ± 0.24	4.94 ± 0.22	4.94 ± 0.22	0.910	0.980	0.980	0.990
Image noise	4.92 ± 0.26	4.90 ± 0.29	4.91 ± 0.29	0.880	0.990	0.990	0.999
Artifact	4.95 ± 0.20	4.94 ± 0.20	4.93 ± 0.24	0.750	0.999	0.811	0.783
Diagnostic acceptability	$4.95 \pm 0.22$	4.93 ± 0.24	4.93 ± 0.23	0.960	0.970	0.970	0.999

**Table 4**. The results of subjective image analysis comparing different image protocols. Data are reported as mean ± standard deviation. *IR* iterative reconstruction; *DLR* deep learning reconstruction; *CE* contrastenhancement.

artifacts due to the appearance of spotty, high-density artifacts in the bowels. The peristaltic and involuntary movement of the bowel challenges the acquisition of subtraction images for the CE-boost<sup>22</sup>.

Our study has some limitations. Firstly, this retrospective study was conducted at a single institution and focused on the radiation dose and image quality of abdominopelvic CT using both quantitative and qualitative analyses. Secondly, patients were scanned using two different CT scanners, although the scanning parameters kept consistent across both scanners. Therefore, a larger study is required to assess the diagnostic performance of DLR and CE-boost with a SilverBeam filter for evaluating other clinical scenarios. In addition, a tube voltage of only 120 kVp was utilized. While using lower tube voltage generally has the advantages of increasing CT

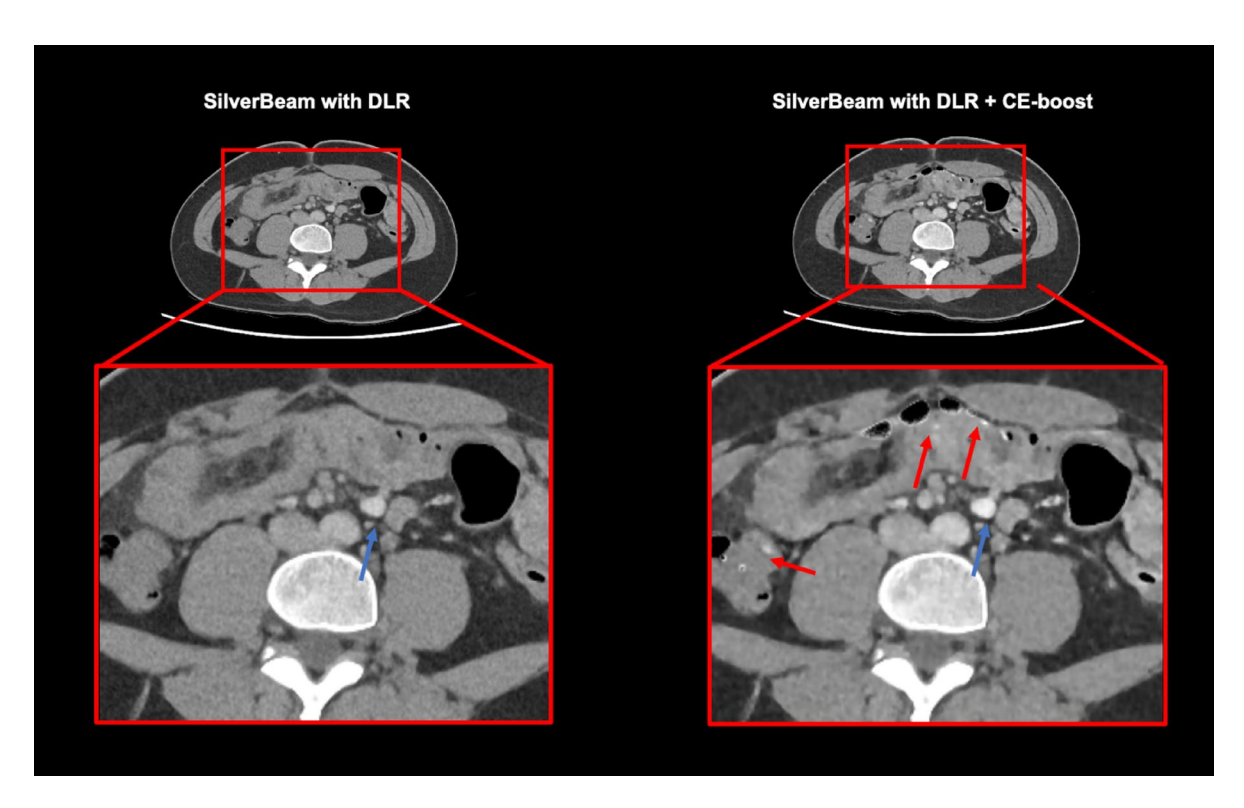


**Fig. 4.** A comparison between reduced-dose computed tomography (CT) with deep DLR images, with and without CE-boost. Although, CE-boost markedly increased CT attenuation (blue arrow) even at reduced dose levels using SilverBeam filter, spotty high-density artifacts (red arrows) were observed in the bowel. These artifacts resulted from misregistration between non-contrast and CE images, exacerbated by motion artifacts. *DLR* deep learning reconstruction; *CE* contrast-enhanced.

attenuation and reducing radiation dose, it was limited by the availability of the SilverBeam filter, which was only compatible with the 120 kVp settings.

In conclusion, DLR combined with a silver filter is effective for routine abdominopelvic CT, achieving a clearly reduced radiation dose while providing image quality that is non-inferior to standard dose with IR. Moreover, the implementation of CE-boost in the reduced radiation dose protocol with DLR yields lower image noise and higher SNR and CNR, compared with standard-dose CT with IR.

### Data availability

The datasets generated during and/or analysed during the current study are available from the corresponding author on reasonable request.

Received: 6 November 2024; Accepted: 8 July 2025

Published online: 16 July 2025

### References

- 1. Pandharipande, P. V. et al. CT in the emergency department: A real-time study of changes in physician decision making. *Radiology* **278**, 812–821 (2016).
- Tsapaki, V. et al. CT diagnostic reference levels based on clinical indications: Results of a large-scale European survey. Eur. Radiol. 31, 4459-4469 (2021).
- 3. Smith-Bindman, R. et al. Radiation dose associated with common computed tomography examinations and the associated lifetime attributable risk of cancer. *Arch. Intern. Med.* **169**, 2078–2086 (2009).
- 4. Lira, D., Padole, A., Kalra, M. K. & Singh, S. Tube potential and CT radiation dose optimization. *AJR Am. J. Roentgenol.* 204, W4-10 (2015)
- 5. Mayo-Smith, W. W., Hara, A. K., Mahesh, M., Sahani, D. V. & Pavlicek, W. How I do it: Managing radiation dose in CT. Radiology 273, 657–672 (2014).
- Szczykutowicz, T. P. et al. CT protocol management: Simplifying the process by using a master protocol concept. J. Appl. Clin. Med. Phys. 16, 228–243 (2015).
- 7. Smith-Bindman, R. et al. Large variation in radiation dose for routine abdomen CT: Reasons for excess and easy tips for reduction. *Eur. Radiol.* **34**, 2394–2404 (2024).
- 8. Choi, E. S., Kim, J. S., Lee, J. K., Lee, H. A. & Pak, S. Prospective evaluation of low-dose multiphase hepatic computed tomography for detecting and characterizing hepatocellular carcinoma in patients with chronic liver disease. *BMC Med. Imaging* 22, 219 (2022).
- 9. Hamberg, L. M., Rhea, J. T., Hunter, G. J. & Thrall, J. H. Multi-detector row CT: Radiation dose characteristics. *Radiology* 226, 762–772 (2003).
- Frush, D. P. et al. Computer-simulated radiation dose reduction for abdominal multidetector CT of pediatric patients. AJR Am. J. Roentgenol. 179, 1107–1113 (2002).

- 11. McCollough, C. H. et al. Degradation of CT low-contrast spatial resolution due to the use of iterative reconstruction and reduced dose levels. *Radiology* 276, 499–506 (2015).
- 12. Jensen, K., Martinsen, A. C., Tingberg, A., Aaløkken, T. M. & Fosse, E. Comparing five different iterative reconstruction algorithms for computed tomography in an ROC study. *Eur. Radiol.* 24, 2989–3002 (2014).
- 13. Volders, D., Bols, A., Haspeslagh, M. & Coenegrachts, K. Model-based iterative reconstruction and adaptive statistical iterative reconstruction techniques in abdominal CT: Comparison of image quality in the detection of colorectal liver metastases. *Radiology* **269**, 469–474 (2013).
- Shuman, W. P. et al. Model-based iterative reconstruction versus adaptive statistical iterative reconstruction and filtered back projection in liver 64-MDCT: Focal lesion detection, lesion conspicuity, and image noise. AJR Am. J. Roentgenol. 200, 1071–1076 (2013).
- 15. Nagayama, Y. et al. Improving image quality with super-resolution deep-learning-based reconstruction in coronary CT angiography. Eur. Radiol. 33, 8488–8500 (2023).
- Nakamura, Y. et al. Deep learning-based CT image reconstruction: Initial evaluation targeting hypovascular hepatic metastases. Radiol. Artif. Intell. 1, e180011 (2019).
- 17. Nam, J. G., Hong, J. H., Kim, D. S., Oh, J. & Goo, J. M. Deep learning reconstruction for contrast-enhanced CT of the upper abdomen: Similar image quality with lower radiation dose in direct comparison with iterative reconstruction. *Eur. Radiol.* 31, 5533–5543 (2021).
- 18. Leyendecker, P. et al. Prospective evaluation of ultra-low-dose contrast-enhanced 100-kV abdominal computed tomography with tin filter: Effect on radiation dose reduction and image quality with a third-generation dual-source CT system. *Eur. Radiol.* 29, 2107–2116 (2019).
- 19. Agostini, A. et al. Third-generation iterative reconstruction on a dual-source, high-pitch, low-dose chest CT protocol with tin filter for spectral shaping at 100 kV: A study on a small series of COVID-19 patients. *Radiol. Med.* **126**, 388–398 (2021).
- Oshima, Y. et al. Capability for dose reduction while maintaining nodule detection: Comparison of silver and copper X-ray spectrum modulation filters for chest CT using a phantom study with different reconstruction methods. Eur. J. Radiol. 166, 110969 (2023).
- 21. Kawamoto, K., Sato, H. & Kogure, Y. Usefulness of Ag additional filter on image quality and radiation dose for low-dose chest computed tomography. *J. Comput. Assist. Tomogr.* **48**, 236–243 (2024).
- 22. Xu, J. et al. Effects of contrast enhancement boost postprocessing technique in combination with different reconstruction algorithms on the image quality of abdominal CT angiography. Eur. J. Radiol. 154, 110388 (2022).
- 23. Otgonbaatar, C. et al. A novel computed tomography image reconstruction for improving visualization of pulmonary vasculature: Comparison between preprocessing and postprocessing images using a contrast enhancement boost technique. *J. Comput. Assist. Tomogr.* 46, 729–734 (2022).
- 24. Iizuka, H. et al. Contrast enhancement boost technique at aortic computed tomography angiography: Added value for the evaluation of type II endoleaks after endovascular aortic aneurysm repair. Acad. Radiol. 26, 1435–1440 (2019).
- 25. Otgonbaatar, C. et al. The effectiveness of post-processing head and neck CT angiography using contrast enhancement boost technique. PLoS ONE 18, e0284793 (2023).
- Sagara, Y. et al. Abdominal CT: Comparison of low-dose CT with adaptive statistical iterative reconstruction and routine-dose CT with filtered back projection in 53 patients. AJR Am. J. Roentgenol. 195, 713–719 (2010).
- Nicolan, B. et al. Diagnostic performance of ultra-low dose versus standard dose CT for non-traumatic abdominal emergencies. Diagn. Interv. Imaging 102, 379–387 (2021).
- Shrimpton, P. C., Wall, B. F., Yoshizumi, T. T., Hurwitz, L. M. & Goodman, P. C. Effective dose and dose-length product in CT. Radiology 250, 604–605 (2009).
- 29. Pearce, M. S. et al. Radiation exposure from CT scans in childhood and subsequent risk of leukaemia and brain tumours: A retrospective cohort study. *Lancet* 380, 499-505 (2012).
- 30. Mathews, J. D. et al. Cancer risk in 680,000 people exposed to computed tomography scans in childhood or adolescence: Data linkage study of 11 million Australians. *BMJ* 346, f2360 (2013).
- 31. Golbus, A. É. et al. Ultra-low dose chest CT with silver filter and deep learning reconstruction significantly reduces radiation dose and retains quantitative information in the investigation and monitoring of lymphangioleiomyomatosis (LAM). Eur. Radiol. 34, 5613–5620 (2024).
- 32. Tamura, A. et al. Deep learning reconstruction allows low-dose imaging while maintaining image quality: Comparison of deep learning reconstruction and hybrid iterative reconstruction in contrast-enhanced abdominal CT. Quant. Imaging Med. Surg. 12, 2977–2984 (2022).
- 33. Hou, J. et al. Clinical application of the contrast-enhancement boost technique in computed tomography angiography of the portal vein. *Abdom. Radiol. (NY)* **48**, 806–815 (2023).

### **Author contributions**

Conceptualization: C. Otgonbaatar, S. H. Jeon, S. J. Cha, H. Shim, J.W. Kim, J.H. Ahn. Data curation: C. Otgonbaatar, S. H. Jeon, S. J. Cha; Formal analysis: C. Otgonbaatar, S. J. Cha; Investigation: C. Otgonbaatar, S. J. Cha, J.W. Kim, J.H. Ahn; Methodology: C. Otgonbaatar, J.H. Ahn; Project administration: H. Shim, J.W. Kim, J.H. Ahn; Resources: S. H. Jeon, S. J. Cha, J.W. Kim, J.H. Ahn; Software: C. Otgonbaatar, S. J. Cha; Supervision: H. Shim, J.H. Ahn; Validation: C. Otgonbaatar, S. H. Jeon, S. J. Cha, H. Shim, J.W. Kim, J.H. Ahn; Visualization: C. Otgonbaatar, S. H. Jeon, S. J. Cha, H. Shim, J.W. Kim, J.H. Ahn; Writing-original draft: C. Otgonbaatar, J.H. Ahn; Writing-review & editing: C. Otgonbaatar, J.H. Ahn. All authors reviewed the manuscript.

### **Declarations**

### Competing interests

The co-authors (C. Otgonbaatar and H. Shim) are employee Canon Medical Systems Korea, Seoul, Korea that is the subsidiary in Korea of Canon Medical Systems Corporation, Otawara-si, Japan.

### Additional information

Correspondence and requests for materials should be addressed to J.-H.A.

Reprints and permissions information is available at www.nature.com/reprints.

**Publisher's note** Springer Nature remains neutral with regard to jurisdictional claims in published maps and institutional affiliations.

Open Access This article is licensed under a Creative Commons Attribution-NonCommercial-NoDerivatives 4.0 International License, which permits any non-commercial use, sharing, distribution and reproduction in any medium or format, as long as you give appropriate credit to the original author(s) and the source, provide a link to the Creative Commons licence, and indicate if you modified the licensed material. You do not have permission under this licence to share adapted material derived from this article or parts of it. The images or other third party material in this article are included in the article's Creative Commons licence, unless indicated otherwise in a credit line to the material. If material is not included in the article's Creative Commons licence and your intended use is not permitted by statutory regulation or exceeds the permitted use, you will need to obtain permission directly from the copyright holder. To view a copy of this licence, visit <a href="http://creativecommons.org/licenses/by-nc-nd/4.0/">http://creativecommons.org/licenses/by-nc-nd/4.0/</a>.

© The Author(s) 2025